



# Centrifuge modelling of folding in high-grade rocks during rifting

Lyal B. Harris<sup>a,\*</sup>, Hemin A. Koyi<sup>b</sup>

<sup>a</sup>*Tectonics Special Research Centre, Department of Geology and Geophysics, The University of Western Australia, 35 Stirling Highway, Crawley 6009, Australia*

<sup>b</sup>*Hans Ramberg Tectonic Laboratory, Institute of Earth Sciences, Uppsala University, Villavägen 16, Uppsala S – 752 36, Sweden*

Received 29 November 2000; revised 17 January 2002; accepted 22 January 2002

## Abstract

Centrifuge modelling is used to simulate the progressive development of structures in a simplified crustal profile during rifting. This paper focuses on folding of ductile layers representing the middle to lower crust. Displacement along a pre-existing cut in the layer representing mantle lithosphere creates a broad shear zone in overlying ductile layers and an asymmetric rift in upper layers. The footwall of the 'mantle lithosphere' layer and overlying shear zone are rotated to sub-horizontal during rise of the basal ductile layer (representing asthenosphere) as an isostatic response to thinning in the extended model. Synthetic and antithetic faults develop in models with thicker ductile 'crustal' layers. Although upper, semi-brittle layers, representing upper crust constitute a simple fault-bounded or sag 'basin', the underlying ductile layers are complexly folded. Open, upright folds developed over the crest of the footwall 'mantle lithosphere' layer are tightened and increased in amplitude as they progressively rotate to a recumbent attitude. Refolding occurs during rise of the basal ductile material representing asthenosphere and from boudinage of overlying competent layers. This study suggests that regional-scale folds in some high-grade terrains previously interpreted as evolving in a convergent margin tectonic setting may instead be produced as a result of flow of the ductile crust during rifting. © 2002 Elsevier Science Ltd. All rights reserved.

*Keywords:* Centrifuge modelling; Crustal profile; Rifting; Folding; Granulites; Amphibolites

## 1. Introduction

This paper presents centrifuge modelling of the progressive development of structures in a layered crust during rifting. Model results have implications for the interpretation of structures in high-grade terrains. Granulite and amphibolite facies rocks frequently contain an early-formed, initially sub-horizontal gneissic foliation folded about isoclinal recumbent folds and refolded by upright to inclined folds (e.g. Escher and Pulvertaft, 1976; Sandiford and Wilson, 1984; Passchier et al., 1990; Boger et al., 2000). Models were carried out to ascertain whether it might be possible for such structures to develop in high-grade rocks during regional horizontal extension. Emphasis is placed on simulating styles and mechanisms of folding in the ductile crust above a pre-existing discontinuity in the upper mantle and due to boudinage of competent layers.

## 2. Modelling method

### 2.1. Simulation of a continental lithosphere

Models (e.g. Fig. 1a) were constructed of materials (Table 1) whose density and viscosity are scaled to replicate a simplified lithospheric strength profile when accelerated at 900–1000 *G* in the large centrifuge (Fig. 1b and c) in the Hans Ramberg Tectonic Laboratory at Uppsala University. Scaling of centrifuge models is discussed by Ramberg (1967, 1973, 1981), Dixon and Summers (1985), and Weijermars and Schmeling (1986). Although individual models have minor changes in layer thickness (Table 2), they are based on predicted lithospheric mechanical properties (e.g. Kuszniir and Park, 1984) where two high strength horizons (the upper crust and upper mantle) are separated by a low strength zone (the middle to lower crust). For ease of referring to layers in the following text, names in inverted commas refer to model layers representing the equivalent feature in nature.

#### 2.1.1. Upper, brittle 'crust'

To enable layer-parallel extension with acceleration

\* Corresponding author. Tel.: +61-9-381-2085; fax: +61-8-9380-1037.

*E-mail addresses:* lharris@tsrc.uwa.edu.au (L.B. Harris), Hemin.Koyi@geo.uu.se (H.A. Koyi).

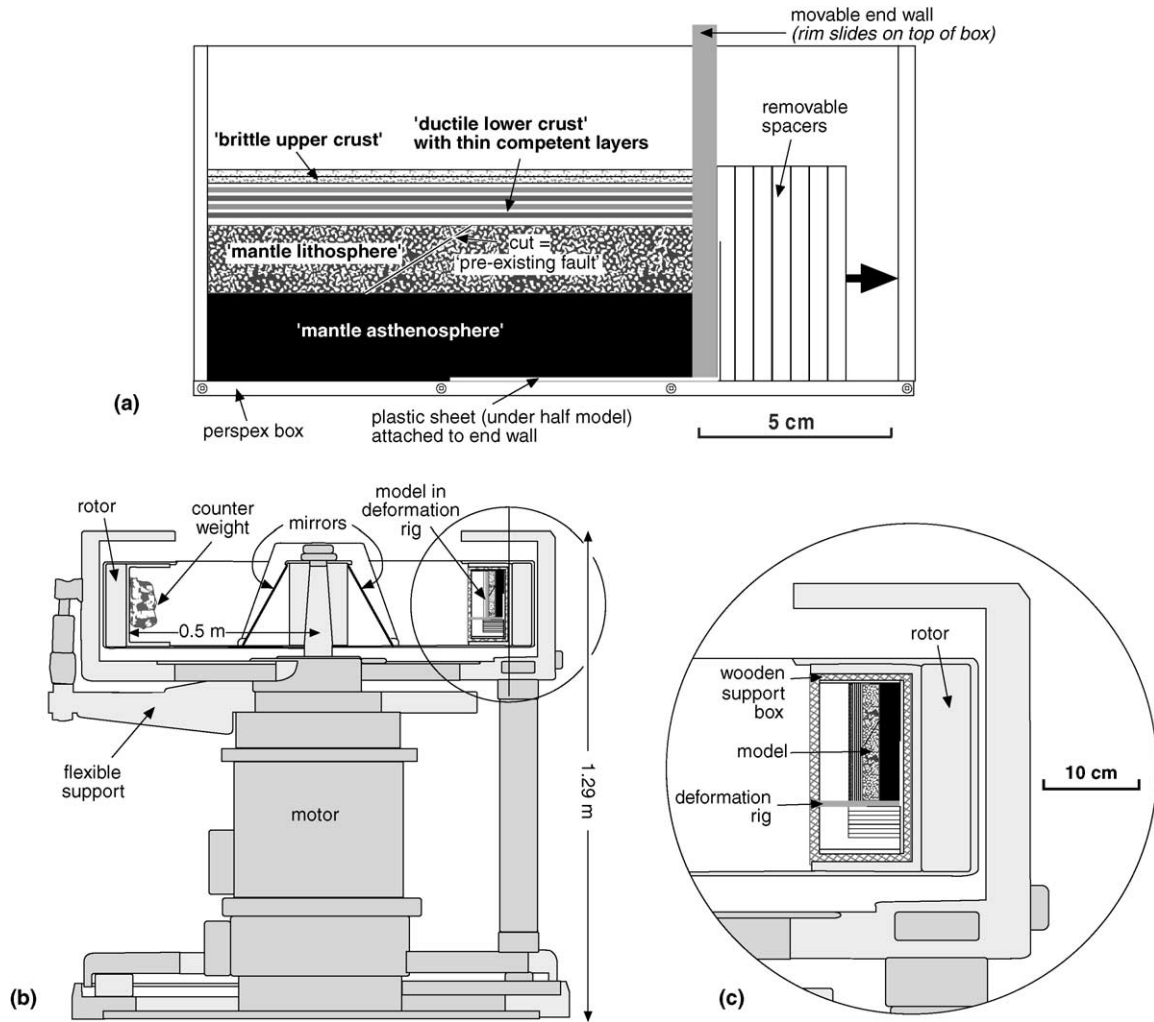


Fig. 1. Analogue model construction and positioning in centrifuge. (a) Model in deformation rig. Removable spacers control increments of extension. See Table 1 for composition of layers and Table 2 for measurements of layer thicknesses for different models. (b) Schematic diagram of the large centrifuge in the Hans Ramberg Tectonic Laboratory, Uppsala University, used for experiments described in this paper (modified after Ramberg, 1981, fig. 10.1). Note that the rig is vertical in the centrifuge, as shown in the enlargement in (c).

Table 1  
Materials used in centrifuge models to represent layers in the lithosphere and asthenosphere

Nature	Modelling material
Upper, brittle crust	Cellulose, glycerine and vaseline paste (cohesive but will fracture) and/or a mix of plastilina and Canderel™ (maltodextrin and aspartam, used to decrease density to $\leq 1.2 \text{ g cm}^{-3}$ ).
Ductile crust	Ductile layers: Dow Corning silicone mixed with $\text{BaSO}_4 \pm$ plastilina to increase density to $1.2 \text{ g cm}^{-3}$ . The effective viscosity at the strain rate of ca. $1.6 \times 10^{-2} \text{ s}^{-1}$ of experiments is ca. $1.5 \times 10^5 \text{ Pa s}$ . Interlayered thin, competent layers: plastilina (density = $1.7 \text{ g cm}^{-3}$ ).
Mantle lithosphere	Plastilina mixed with Canderel (density = ca. $1.4 \text{ g cm}^{-3}$ ).
Mantle asthenosphere	Silicone putty, plastilina and iron oxide (to increase density to $1.46 \text{ g cm}^{-3}$ ) and acid oil (to decrease its effective viscosity to ca. $3 \times 10^5 \text{ Pa s}$ ).

acting normal to layers, the deformation rig (Fig. 1a) is positioned in the centrifuge so that the layers are vertical (Fig. 1b and c). Unconsolidated sand or other granular materials (as reviewed by Schellart, 2000) commonly used to simulate upper crustal rocks could not be utilised in our

Table 2  
Initial thicknesses of layers and dip of prescribed cut through mantle lithosphere for each model

Layer	Model 1	Model 2	Model 3	Model 4
Layer thickness (mm)				
Upper crust	4	2	2	3
Lower crust	9	8	7.6	10
Mantle lithosphere	12	12	11	10
Dip of prescribed cut in mantle lithosphere (°)				
	45	30	45	50

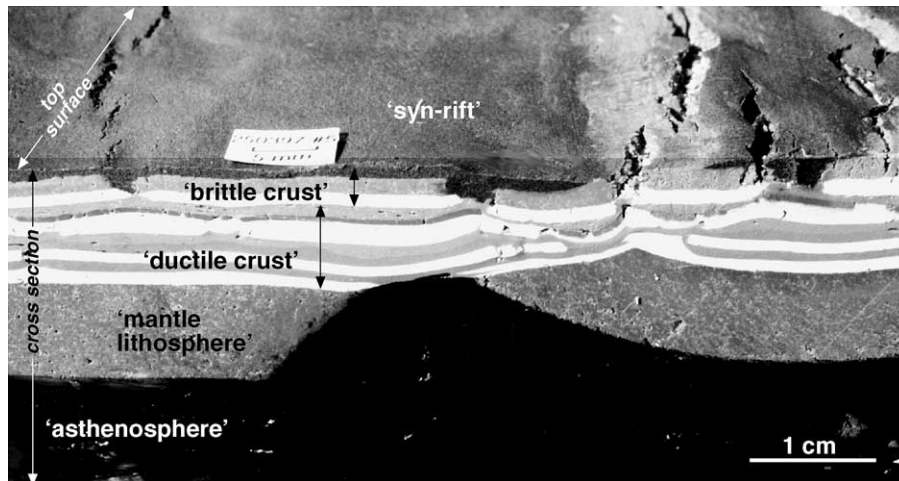


Fig. 2. Oblique photograph of Model 3 showing development of an asymmetrical rift. Note normal displacement and separation along the prescribed cut in the layer representing mantle lithosphere, with uplift and rotation to a shallower dip of its footwall. The basal 'asthenosphere' layer has flowed between the separated 'lithospheric mantle' layer. In nature, normal faults may develop in positions where upper brittle layers have fractured.

experiments due to the vertical positioning of the deformation rig and the requirement that models were to be sliced and reassembled after successive increments of extension. Cohesive upper layers are thus required to model the brittle crust in the apparatus used and problems were encountered in finding an ideal analogue. Although several substances were tested, no material was found that was equal or less dense than underlying layers and that would fail by shear fracturing under the imposed modelling conditions. Plastilina modelling putty (a Swedish modelling putty whose physical properties have been described by Weijermars (1986), which is similar to Plasticine described by McClay (1976)) mixed with Canderel (a fine-grained maltodextrin and aspartame powder, added to decrease density to that of underlying ductile layers or less) was found to be the best material to simulate a semi-brittle upper crust. Although open fractures develop in this material instead of faults during layer-parallel extension (Fig. 2), their position may be taken as an indication where normal faults may form in nature. Layers of a mix of acetate powder and Vaseline and/or glycerine and plaster of Paris (both of which also formed tensile fractures) were applied at successive stages of rifting in down-thrown areas of the models to represent syn-rift sediments. Despite the inability to model upper crustal fault geometries precisely using these materials, the general form of sedimentary basins and localisation of syn-rift sequences can be ascertained. This representation of the upper crust was adequate for our experiments whose main purpose was to model the evolution of structures in the underlying ductile crust.

### 2.1.2. Ductile 'crust'

The extreme reflectivity and laminated structure of the middle to lower crust commonly observed in deep seismic profiles is best explained if it is compositionally heterogeneous (Meissner and Wever, 1986; Reston, 1990; Wernicke,

1990). These authors propose a rheological stratification of alternating strong (e.g. mafic or ultramafic) and weak/low viscosity (e.g. quartzo-feldspathic or 'wet-quartz') zones. Strength profiles that show the alternation of weak and strong zones with depth in the middle to lower crust (e.g. Zuber et al., 1986; Kruse et al., 1991) generally provide a better match to deep seismic data and field exposures of high grade terrains than those where only the lowermost crust is portrayed as a thin viscous channel (e.g. Hopper and Buck, 1996). Ductile flow within weak layers in the middle to lower crust exerts an important control on deformation of the continental lithosphere (Wernicke, 1990; Ranalli, 1997). Ductile flow in the lower crust is thought to be highly heterogeneous (see Ranalli, 1997 and citations therein).

In our experiments, Dow Corning Rhodorsil Gomme (whose composition and properties are described by Weijermars, 1986) silicone putty layers simulate weaker zones in which ductile flow can occur in the middle to lower crust. The density of the silicone was increased to  $1.2 \text{ g cm}^{-3}$  by adding barytes ( $\text{BaSO}_4$ ) and layers were coloured using powdered pigment. Flow properties of this composite material are given in Fig. 3. The fluid-like flow of rocks and analogue materials can be expressed as a power law (Weijermars, 1986):

$$\dot{\gamma} = A\sigma^n$$

where  $\sigma$  = stress,  $\dot{\gamma}$  = strain rate, and  $A$  = a constant. At strain rates greater than ca.  $0.1 \text{ s}^{-1}$ , the silicone-barytes mix behaves in a Newtonian manner (i.e.  $n = 1$ ) with a viscosity of  $10^5 \text{ Pa s}$ . At lower strain rates, the composite material deforms as a power law fluid with exponent  $n = 1.5$  (possibly increasing to ca. 2.6 at strain rates lower than ca.  $0.01 \text{ s}^{-1}$ , although more data is required to confirm this). These results are comparable with studies of composite silicone-barytes mixes by Weijermars (1986). The strain rate

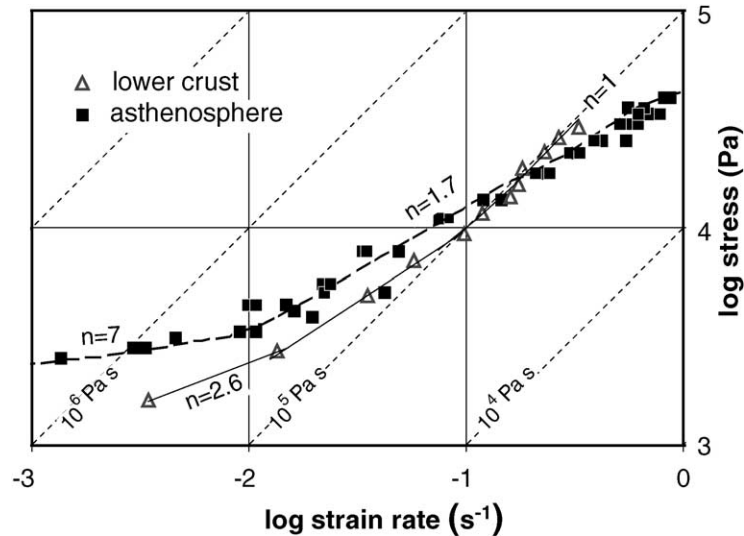


Fig. 3. Flow properties of the Rhodosil Gomme–iron oxide–acid oil mix used to represent the asthenosphere and Dow Corning 3179 Dilatant Compound silicone putty–barytes mix used to model the ductile crust. Data calculated using spaghetti and annular shear viscometers.

in our experiments was ca.  $1.6 \times 10^{-2} \text{ s}^{-1}$ . At this strain rate, the effective viscosity (Weijermars, 1997) of the material used for the ductile lower crust is  $1.5 \times 10^5 \text{ Pa s}$ . Embedded thin layers of Plastilina ( $n = \text{ca. } 9.5$ ; Weijermars, 1986) represent competent layers within the ductile matrix.

### 2.1.3. 'Mantle lithosphere'

The upper mantle in continental lithosphere represents a strong, load-bearing layer except for cases of extreme heat flow (Ranalli, 1997). There is a large variation in thicknesses determined for both the crust and mantle lithosphere, with crustal thickness generally being greater for older lithosphere (Meissner and Wever, 1988; Fernández and Ranalli, 1997; Ranalli, 1997; Artemieva and Mooney, 2001; Poudjom Djomani et al., 2001). Whilst the mantle lithosphere is generally thicker than the crust, in some cases it is considered to be thinner (e.g. Kruse et al., 1991; Fernández and Ranalli, 1997, fig. 1). This may be especially the case for Palaeozoic lithosphere. Buck (1991) and Hopper and Buck (1996) show that changing the relative thickness of mantle lithosphere to crust may change the width and structural styles of rift zones. Models where the mantle lithosphere was both thicker and thinner than the crust were therefore built (Table 2). A relatively thin mantle lithosphere was used in analogue models of Benes and Davy (1996).

Evidence for the localisation of deformation in the upper mantle into shear zones during rifting comes from field studies of exhumed mantle rocks (e.g. Vissers et al., 1995, 1997). Vissers et al. (1995) conclude that shear localisation may have resulted in a drastic decrease in strength of the upper mantle during rifting. Reflections in the upper mantle on deep seismic profiles offshore Britain have been interpreted as localised shear zones (Warner and McGeary,

1987; Klemperer, 1988; Reston, 1990, 1993; Brun and Tron, 1993). The Moho is displaced by as much as 40 km along such structures (Brun and Tron, 1993). Shear zones displacing the upper mantle are generally thought to represent the extensional reactivation of former subduction zones (e.g. Phinney, 1986; Mooney and Meissner, 1992; Reston, 1993). Govers and Wortel (1993, 1995) contend that a pre-existing weak zone in the upper mantle is required for asymmetric lithospheric deformation involving the upper mantle to occur. Koyi and Skelton (2001) used centrifuge models to show that a pre-existing 'fault' localises deformation during extension and leads to rotation of high-angle normal faults to shallower dips, producing low-angle detachments.

In our models, lithospheric mantle was treated as a competent, brittle–ductile layer and was modelled using plastilina mixed with Canderel. Fernández and Ranalli (1997) suggest that dynamic models need initial perturbations, such as pre-existing faults, in order to concentrate deformation in a finite area. In order to localise structures within the ductile crust in an asymmetric rift and to replicate the displacement along an upper mantle shear zone (as in the examples cited above), an inclined cut was made through the model's 'mantle lithosphere' layer.

### 2.1.4. 'Asthenosphere'

A ductile basal layer was used to represent the asthenosphere. This was modelled using Rhodosil Gum silicone putty mixed with fine magnetite powder and plastilina to increase its density to  $1.42 \text{ g cm}^{-3}$  and acid oil to decrease its effective viscosity to ca.  $3 \times 10^5 \text{ Pa s}$  for the strain rate used in experiments. Flow properties are given in Fig. 3. This composite material is non-Newtonian at all strain rates tested, changing from  $n = 1.7$  at strain rates greater than  $0.01 \text{ s}^{-1}$  (i.e. as in our models) to  $n = 7.1$  at lower strain rates.

## 2.2. Technique

The models were constructed of layers rolled to the constant desired thickness, frozen to facilitate handling, and placed in a perspex box with one end wall free to move (Fig. 1a). The thicknesses of layers for each model are provided in Table 2. A thin film of clear PDMS, a low viscosity silicone (Weijermars, 1986) was applied to the end- and side-walls of the model to reduce frictional ‘drag’ as the model is thinned during extension. A narrow block of plastilina upon a viscous block of a silicone–plastilina–barytes–gypsum mix constrained the edges of the more ductile material representing asthenosphere. After returning to room temperature (approximately 20 °C), the rig was positioned vertically in the centrifuge (Fig. 1b and c). A counterweight of equal mass was used to balance the rotor arm (Fig. 1b). Models extended parallel to the initial compositional layering (i.e. vertically in the centrifuge) as a response to the applied acceleration of between 900 and 1000 *G* acting normal to the layers. Removing spacers (Fig. 1a) controlled increments of extension. Experiments thus represent a passive style of rifting in an overall pure shear setting, with thinning of model layers representing continental lithosphere and up-welling of the basal material representing mantle asthenosphere.

Typical experiments consisted of 7–12 runs, each of 2–10 min duration. Models were partially frozen, sliced and photographed at different stages of deformation to record the progressive development of structures. After slicing, the models were reassembled in the deformation rig and left to return to room temperature upon which silicone layers fused together. After further extension, new slices were made, away from the previous cut, as plastilina layers do not rejoin after slicing (no reactivation of cuts was, however, observed after subsequent extension). Details of model slices presented in this paper have been traced from photographic enlargements (black-and-white photographs are not included, as individual layers are not readily distinguishable).

## 3. Results

### 3.1. Model 1

Model 1 (Fig. 4) shows the progressive development of structures during rifting where there is a moderately dipping initial cut through the mantle lithosphere layer (subsequently referred to as the ‘mantle shear zone’). At early stages of rifting, ductile layers and boudinaged competent plastilina horizons are displaced in a normal sense within a broad shear zone that has propagated from the prescribed cut in the ‘mantle lithosphere’ through the ‘ductile crust’ (Fig. 4a and c). An early-formed antithetic shear zone (dipping towards the rift axis) with a lesser throw and limited strike extent is restricted to the ‘middle crust’

(Fig. 4a). Minor antithetic shear zones also form in the middle and uppermost ductile ‘crustal’ layers above the ‘mantle lithosphere’ footwall at higher strain (Fig. 4e and g).

Uplift of the upper corner of the ‘lithospheric mantle’ footwall occurs during displacement on the mantle shear zone. This results in a characteristic triangular crest (seen in all experiments) defined by the initial cut through the ‘mantle lithosphere’ layer that dips towards the axis of rifting, and the sloping surface away from the rift of the uplifted footwall (Fig. 4a–e). With increased extension of the model, there is an increased displacement on the ductile shear zone and a rotation and flattening in dip of the pre-existing ‘mantle shear zone’ (Fig. 4e and g). The footwall ‘mantle lithosphere’ has also necked early in the deformation history (Fig. 4a), reducing its thickness by up to half. This indicates that deformation in the ‘mantle lithosphere’ layer is not restricted to displacement on the mantle shear zone.

Changes in the shape and position of an up-welled ‘asthenospheric bulge’ with time are also apparent. The material representing the asthenosphere has bowed upward, forming a broad arch beneath the thinned, neck area of the ‘mantle lithosphere’ footwall (Fig. 4a). Maximum uplift has occurred beneath the triangular crest in the ‘mantle lithosphere’ footwall. With increased extension, the ‘mantle lithosphere’ has been pulled apart. Separation results in additional up-welling of the ‘asthenosphere’ and migration of its highest point from within the zone of initial separation (Fig. 4c) to immediately adjacent to the rotated ‘mantle lithosphere’ footwall (Fig. 4e–h).

Although there has not been any faulting in the ‘upper crustal’ layers in the early stages of extension, they have been down-warped. The deepest part of this early ‘basin’ (Fig. 4a) is offset towards the hanging-wall side of the ‘mantle shear zone’. With increasing displacement along the mantle shear zone, a broad depression analogous to a sag basin in nature is developed in the ‘upper crust’ (Fig. 4c). This depression is filled to represent syn-rift sediments. The deepest part of the ‘basin’ is now above the separated ‘mantle lithosphere’ (where the ‘asthenosphere’ is shallowest). At the final stage of rifting (Fig. 4g and h), the deepest part of the ‘basin’, that also correlates with the greatest thickness of the earliest ‘syn-rift sediments’, is situated above the mid-point between the two separated segments of the ‘mantle lithosphere’. The deepest part of the upper ‘syn-rift sediment’ layer, however, lies directly above the highest point of the ‘asthenosphere’ that is closer to the footwall ‘mantle lithosphere’ block. Further details of changes in rift basin geometry with time and implications of models for basin evolution are described by Koyi and Harris (2001).

Model 1 clearly shows the progressive development of folds in the lower ‘ductile crust’ layers. The process starts when an inclined fold (verging towards the downthrown block) is formed in the lowermost ‘ductile crust’ layer (layer 1; Fig. 4b) over the triangular crest in the uplifted

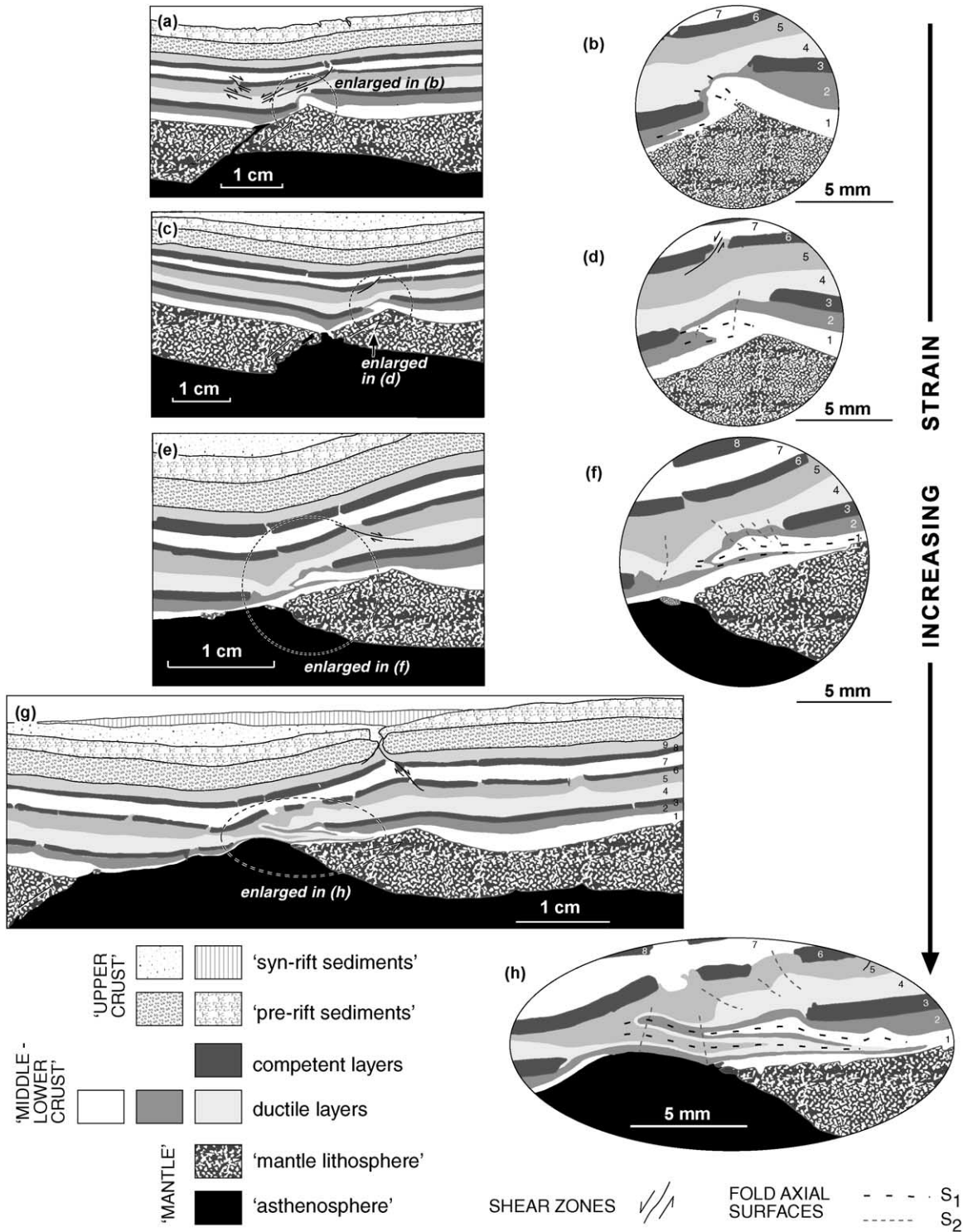


Fig. 4. Model 1 line drawings (traced from photographs) of progressive changes with increasing strain. See text for details. (b), (d), (f) and (h) are enlargements of the circled areas in (a), (c), (e) and (g), respectively, which show the progressive development of folds above the uplifted crest of the 'mantle lithosphere' footwall after 24, 29, 39 and 43% extension. Note refolded isoclinal recumbent folds in lower ductile layers in (g), enlarged in (h), whereas a simple sag basin has developed in the upper crust.

'mantle lithosphere' layer and within the boudin neck of the competent, plastilina horizon (layer 3). In contrast, the second ductile layer from the base has been thinned in the boudin neck, over the fold crest in layer 1 (Fig. 4b). Down-

dip of this fold, layer 1 has thinned due to shearing directly above the mantle shear zone (Fig. 4a). A minor, overturned isoclinal fold that deforms both the two lowermost ductile layers is also developed within the shear zone (Fig. 4b).

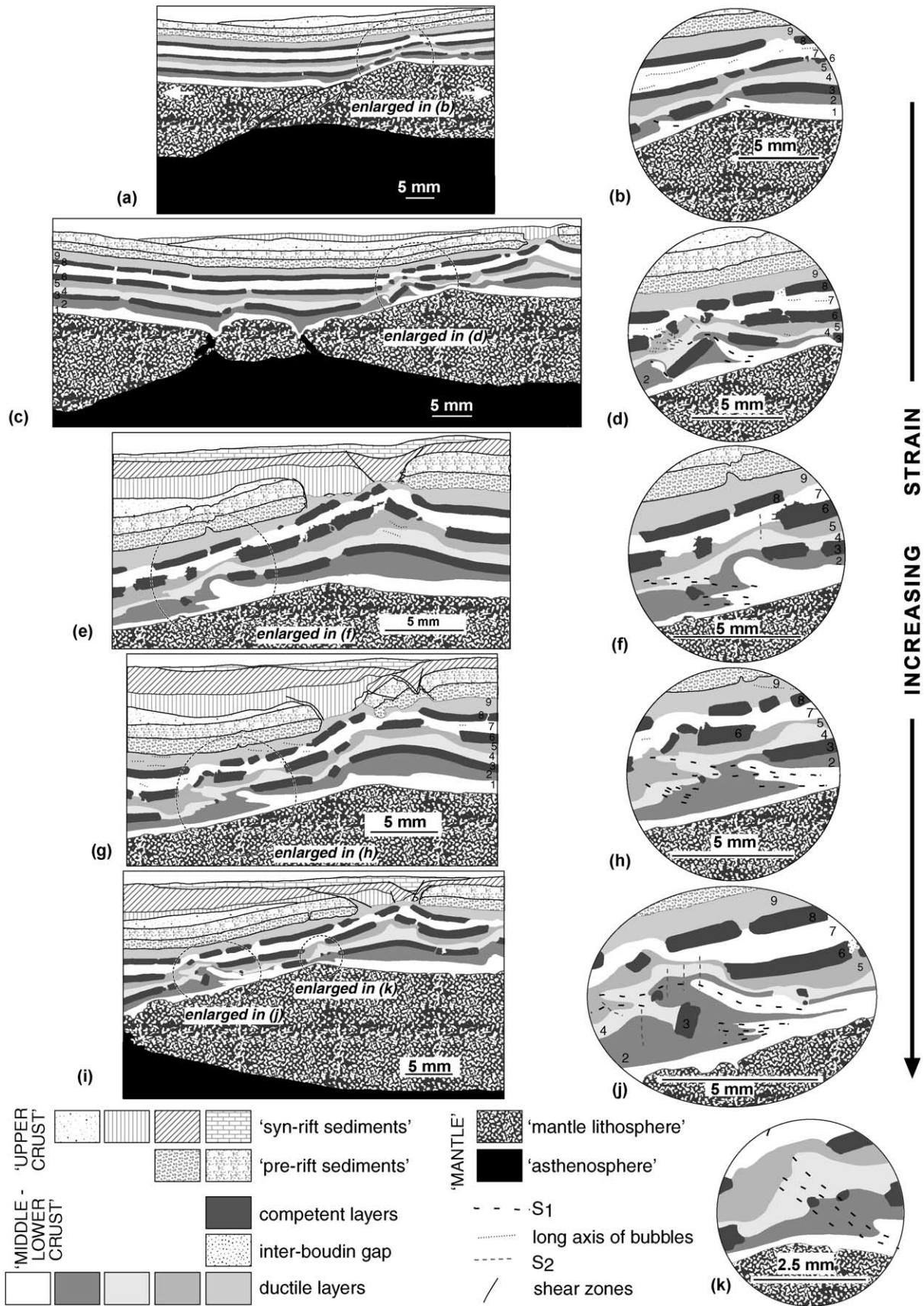


Fig. 5. Model 2. Progressive development of folds and their subsequent refolding in layers representing middle to lower crust. This model commenced with a shallower dip of the prescribed cut through the mantle lithosphere layer. See text for details. (a,b) 37% extension. (c,d) 54% extension. (e–k) Three slices and their enlargements after 57% extension.

With further extension, the axial surface of the main (upper) fold in layer 1 has rotated to horizontal and its upper limb is folded by a symmetrical, upright antiform (Fig. 4d). This antiform (formed due to flow of ductile layers in the boudin neck) is slightly offset towards the downthrown block from the triangular crest of the mantle footwall. At higher strain, the overturned limb of layer 1 is displaced as a fold nappe over layer 2. Inclined folds ( $F_2$ ; Fig. 4f) have refolded the uppermost limb of the previously formed recumbent ( $F_1$ ) fold. The most complex region exists in the area of thinnest 'ductile crust' between the area of greatest 'mantle asthenosphere' uplift and the mid-point of the footwall 'mantle lithosphere' (which has been rotated to a very shallow dip). Here lower crustal flow has resulted in isoclinal recumbent folds of thinned lower crust layers (Fig. 4h). A disharmonic geometry results, as the basal layers were already intensely deformed prior to folding of layers 4 and 5 ( $F_2$  in Fig. 4h). The position of  $F_2$  folds appears in part to be controlled by boudinage of the overlying competent layer. Layer 1 has undergone extreme thinning over the antiformal, up-welled 'mantle asthenosphere', disappearing completely over the crest of the antiform so that layer 2 is in direct contact with the mantle asthenosphere. Layers 2 and 4 (in contact with each other due to boudinage of layer 3) have been twice repeated by recumbent folds.

In addition to the above structures, upright folds have also developed due to several different mechanisms. The isoclinal folds described above have been refolded by upright folds (e.g. Fig. 4h) due to 'asthenospheric' uplift on the margin of the 'mantle lithosphere' footwall block. An upright fold in the wide boudin neck of layer 3 (Fig. 4f) has also folded layers 2, 4 and 5. This fold may be due to displacement on a normal shear zone in the 'mid-crust'. Broad upright, open folds also form between boudin necks away from the rift zone (e.g. layers 4 and 5; right side of Fig. 4g).

### 3.2. Model 2

Model 2 (Fig. 5) has a thinner 'ductile crust' than Model 1, a shallower dip of the cut through the 'mantle lithosphere' (the 'mantle shear zone') and a slightly thicker 'mantle asthenosphere' layer (see Table 2 for model parameters). Fig. 5a shows an early stage after normal displacement along the mantle shear zone. A broad ductile normal shear zone (which steepens upward) extends across the entire 'ductile crust' from the 'mantle shear zone'. At low strains, a broad sag basin is formed (Fig. 5a). In contrast to Model 1, there has been only a slight isostatic uplift of the 'mantle lithosphere' footwall for a similar amount (ca. 37%) of extension (i.e. creation of a smaller crestal triangular zone than in Model 1). A competent plastilina layer (layer 3) is boudinaged above this crest (Fig. 5b). An antithetic normal shear zone, across which plastilina layers have been separated and displaced, is developed over the 'mantle lithosphere' footwall, dipping away from the rift axis (Fig. 5a and e).

There is no horizontal separation of the 'mantle litho-

sphere' layer in early stages of extension (Fig. 5a). After further extension, the upper part of the hanging-wall 'mantle lithosphere' is boudinaged and the dip of the 'mantle shear zone' flattened (Fig. 5c). Fig. 5c also shows the development of minor antithetic shear zones in the 'ductile crust'. The 'brittle crust' has fractured on the basin margin over the synthetic shear zone, and sagged over the system of minor antithetic shears. A broad zone of 'asthenospheric' uplift underlies the entire rift, and thin slivers of 'asthenosphere' have risen to infill the 'lithospheric' boudin gaps (Fig. 5c). There has also been flow of the lower two ductile layers into the upper part of the boudin necks of the competent 'lower crustal' layers. A symmetrical basin is thus formed, where both the deepest 'syn-rift sediments' and brittle 'crustal' layers overlie the shallowest 'asthenosphere'.

Deformation in the deeper, ductile 'crust' is, however, asymmetric and within a broad diffuse zone. This zone extends upwards into the brittle 'crust' above, and up-dip from, the rotated 'mantle lithosphere' shear zone (footwall of the prescribed cut). Uplift of the upper 'ductile crust' (layers 7–9) has occurred beneath this zone, with commensurate flow of the middle 'crust' (layers 4 and 5) to form an antiform underlying the rift margin (Fig. 5e, g and i). Folding is partly due to bending of the competent lower 'crustal' units above the apex of the triangle crest in the 'mantle lithosphere' layer (see Fig. 5f). Conjugate (i.e. antithetic) normal faults above the antiform affect both the brittle crust and syn-rift sediment layers.

Structures created within the zone of intense ductile deformation over the 'mantle lithosphere' footwall increase in their complexity with increasing extension (best seen in enlarged areas in the right of Fig. 5). Complex isoclinal folds with variable fold profiles (from broad, very rounded and overturned to tight, angular and recumbent) have developed. Boudin segments within the normal shear zone have been rotated during flow of the ductile lower 'crustal' layers (Fig. 5d). Ductile layers in the lower to middle 'crust' have been folded into large overturned to recumbent folds. The fold vergence is towards the centre of the rifted 'mantle lithosphere', consistent with a normal sense of shear along the rotated 'mantle lithosphere' footwall. The variability in both the position and style of folds on different slices through the model indicates that folds developed along the basal shear zone to the ductile crust are non-cylindrical. Recumbent folds in the left of Fig. 4j have been refolded about an upright antiform. Folds near the triangular crest of the 'mantle lithosphere' in Fig. 5g and k are similar to those formed in early stages of extension (Fig. 5a).

### 3.3. Model 3

Model 3 was constructed with an even thinner ductile 'crust' (Table 2). This model shows greater development of an antithetic shear zone displacing upper 'crustal' layers and flattening in dip into the upper to middle ductile 'crust' (Fig. 6a). Early stages of deformation were similar to Model



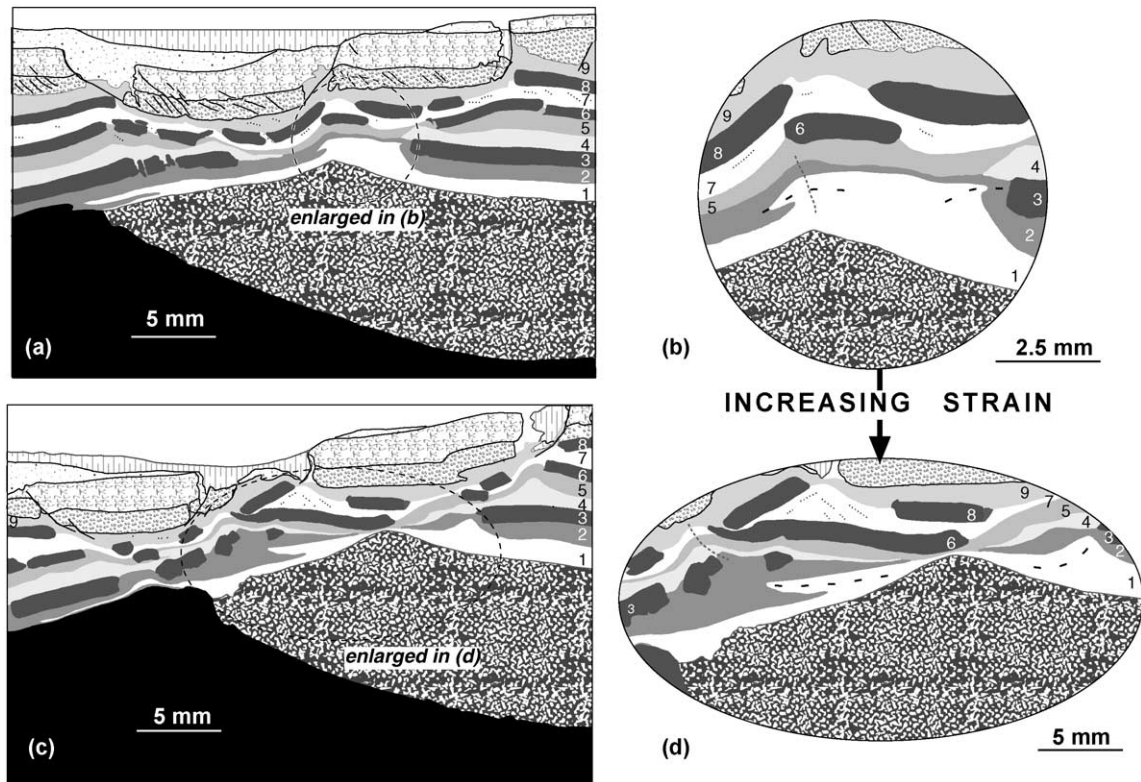


Fig. 6. Model 3, showing two stages in the formation of folds above the flattened 'mantle lithosphere' footwall, and the development of domes in ductile 'crustal' layers beneath a more symmetrical rift. Note normal faulting both on rift margins and above the crest of the rotated 'mantle lithosphere' layer. Legend as for Fig. 5. (a) 55% extension. (b) 66% extension.

1 and again resulted in complete separation of the 'mantle lithosphere' layer. A normal shear zone is formed, extending from the uplifted 'mantle lithosphere' footwall to a steeper dip through the brittle 'crust'. A narrower, symmetrical basin bounded by faults on both margins develops (Fig. 6a). A second, synthetic shear zone is developed over the triangular crest of the 'mantle lithosphere' layer (Fig. 6a), and this structure becomes the basin-bounding structure at higher extension (Fig. 6c).

Open folds are created due to ductile drag into both synthetic and antithetic shear zones. A recumbent isoclinal fold is formed in the two lowermost ductile layers in a zone of intense shear immediately overlying the 'mantle lithosphere' footwall (left side of Fig. 6a). A flat topped fold formed over the triangle crest of the uplifted 'mantle lithosphere' (Fig. 6a and b). Minor folds on the two ends of this structure have opposite vergence. Fig. 6c and d show that the initially flat-topped fold has been dragged into the broad, normal shear zone above the 'mantle lithosphere' footwall, producing a recumbent fold. Note thinning of layers 1–5 over the crest of the uplifted 'mantle lithosphere' layer (Fig. 6d).

### 3.4. Model 4

Model 4 (Fig. 7) differs from the other models due to the 'mantle lithosphere' failing along an irregular surface

instead of along a pre-existing cut. Ductile crustal layers are displaced in a broad shear zone with normal drag of layers across the shear zone (Fig. 7a and e). A steep normal fault offsetting the brittle 'crust' represents a continuation of this shear zone. Minor synthetic and antithetic faults are also developed in the brittle 'crust'. In the early stage of deformation, there has been no uplift of the upper ductile 'crust' on the rift margin. Middle ductile 'crustal' layers (layers 4 to 5 and 7) have been arched upwards to produce a broad antiform below the rift margin in the brittle 'crust'. Ductile crust in the crest of the antiform is at a higher level than the adjacent brittle crust (Fig. 7a). This is a similar process to the formation of a metamorphic core complex or gneiss dome, however only the upper to middle 'crust' is involved in its formation. The antiform dies out with depth, with its centre situated above sub-horizontal lower 'crust' that shows little deformation. Unlike simple shear models for core complex formation, the antiform of deeper 'crustal' layers occurs away from the area of up-welling 'mantle asthenosphere'. An antithetic normal shear zone has also been formed on the flanks of the rising 'asthenosphere' (whose summit is higher than the base of the 'mantle lithosphere'). Layer 1 has thinned across the rotated 'mantle lithosphere' footwall (Fig. 7e), and has been removed over the footwall and domed 'mantle asthenosphere' (Fig. 7a and e). Layer 2 of the lower crust is thus in contact with the

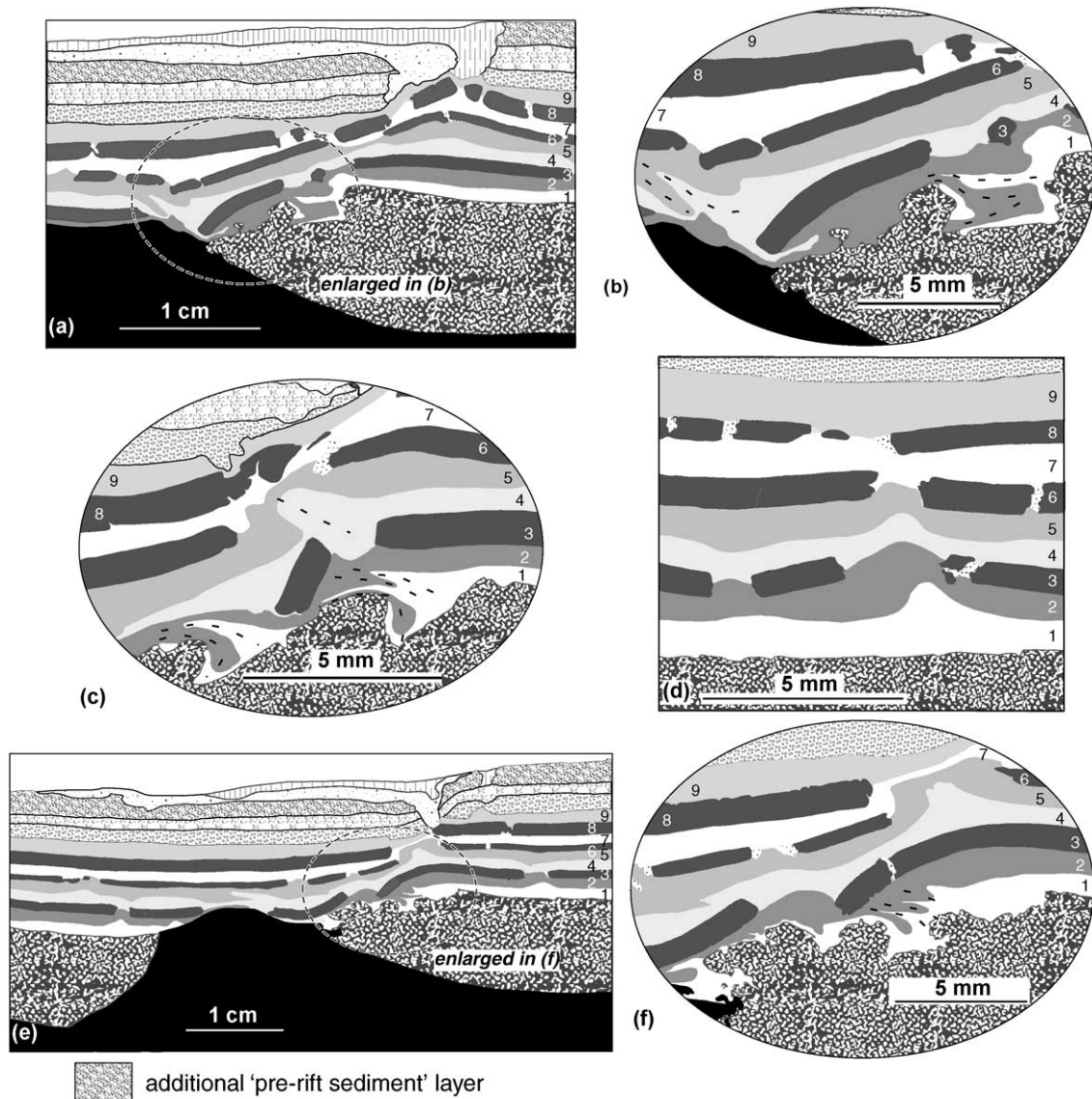


Fig. 7. Model 4. (a–c) and (e,f). Formation of folds due to lower ‘crustal’ flow over an irregular ‘mantle lithosphere’ footwall surface. (a–d) 44% extension, (e,f) 48% extension. (d) Folding between boudinaged competent horizons above a flat lying ‘mantle lithosphere’ layer away from the main zone of rifting. See text for details. Legend as for Fig. 5.

‘asthenosphere’. Complex refolded isoclinal folds are developed in basal ductile layers over the irregular ‘mantle lithosphere’ footwall (Fig. 7b, c and f). Folds are also developed in ductile layers between boudins away from the main rift axis (Fig. 7d).

#### 4. Comparison with other model studies

##### 4.1. Analogue models

Analogue models of lithospheric and upper mantle deformation during rifting under normal laboratory (i.e. 1 G) conditions by Brun and Beslier (1996) show complex strain patterns that suggest a combination of pure and simple shear. In their experiments, necking of the lithosphere

resulted in an overall symmetrical or pure shear pattern of structures, where asymmetric structures developed internally and at higher amounts of extension. The sequential development of structures envisaged by these authors involves formation of early conjugate normal faults within the brittle, upper mantle layer. With increasing strain, displacement was concentrated on one of these faults with continued up-welling of the ductile mantle asthenosphere. In the lower crust, strain was accommodated by ductile flow within shear zones. The sense of shear was top towards the rift axis. At higher extension, the mantle lithosphere is boudinaged, resulting in unstable and asymmetric structures during high amplitude stretching. Continued rising of the ductile mantle occurs with shear zones along the interface between ductile and brittle mantle, with the sense of shear being top away from rift axis. Eventually the ductile mantle

is exhumed in this process. Footwall uplift of the mantle lithosphere layer is greater in our models and plays a greater role in shear zone development in the layers representing the lower crust than those described by Brun and Beslier (1996). The models of Brun and Beslier (1996) only effectively reproduce strength, and not density contrasts. In comparison with the early symmetrical, ‘top towards the zone of mantle uplift’, senses of shear in the models of Brun and Beslier (1996), our asymmetrical centrifuge models show shearing (directed towards the zone of ‘mantle’ uplift) is greatest above the rotated ‘mantle lithosphere’ footwall. Only minor displacement took place on conjugate, antithetic shears (e.g. Fig. 6b). This is comparable with later stages of Brun and Beslier’s (1996) models where deformation in the lower crust changes to a simple shear regime following boudinage of the mantle lithosphere.

Fossen and Rykkelid (1992) describe 1-*G* experiments on folding within ductile layers above a rigid basement block displaced along a normal fault. Although designed to simulate deformation within heterogeneously layered gneiss at the outcrop scale in an extensional detachment, the fault geometry in the basal block in their models is similar to the prescribed cut through the layer representing mantle lithosphere in our experiments. Fossen and Rykkelid (1992) applied large layer-parallel shear strains pre-, syn- and post- displacement on the basal fault. Synchronous normal faulting and layer parallel shear produced folds in ductile layers above the normal fault with moderately dipping axial surfaces, and axes parallel to the strike of the fault. Both natural examples and model results show similarities to the folds in our models, although at less extension. In our models, ductile flow is greatest within the rift zone as a result of displacement along the prescribed cut, whereas both the examples and experiments of Fossen and Rykkelid (1992) have a greater magnitude of layer-parallel shear imposed across the entire zone. Folds formed above irregularities in the basal shear zone in Model 4 are similar to those produced in 1-*G* experiments of spreading nappes by Brun and Merle (1988).

A similar behaviour of a semi-brittle layer overlying a ductile layer to that of the layer used to represent mantle lithosphere in our models is seen in the centrifuge analogue models of low-angle detachment faults by Koyi and Skelton (2001). A pre-existing cut in a semi-brittle layer in their models (representing an initial, high-angle normal fault) is flattened in dip during the rise of the underlying ductile layer, even where the ductile layer was denser.

#### 4.2. Numerical models

Upwards bending of the ‘mantle lithosphere’ as developed in our models has also been portrayed by Buck (1988) and Buck et al. (1988) based on the regional isostatic response to normal fault motion. The geometry of structures produced in our models is very similar to finite element models of Keen and Boutilier (1990) and Boutilier and

Keen (1994). In these models, an initial fault in the upper crust *without* a pre-existing weakness in the mantle lithosphere has resulted in a large amount of normal shear in the upper mantle during horizontal extension. The ensuing uplift and rotation of the footwall to the mantle lithosphere shear, and eventual necking and separation of the mantle lithosphere, took place in the same manner as in our centrifuge models. Numerical modelling by Govers and Wortel (1995) incorporating strain weakening in the lithospheric mantle during extension has also produced normal shear zones in the upper mantle.

## 5. Discussion

### 5.1. Summary

Lower crustal flow during rifting has previously been thought to be a major controlling factor on deformation in the brittle, upper crust (e.g. Melosh, 1990; Wernicke, 1990; Westaway, 1998; Gartrell, 2000). Our centrifuge modelling suggests that lower crustal flow during rifting may also produce complex fold geometries in high-grade rocks that may have previously been interpreted as forming in a thrust tectonic setting.

The geometry of structures in the lower ductile ‘crustal’ layers (especially above the rotated ‘lithospheric mantle’ footwall) is asymmetric, with a sense of shear towards the rift axis. Deformation has not, however, been concentrated into a discrete shear zone that transects the ‘lithosphere’, as portrayed in simple shear rift models such as Wernicke (1985) or Lister et al. (1986, 1991). Instead, strain has been partitioned into deformation along discrete structures in the upper brittle ‘crust’ and ‘mantle lithosphere’, and within a broad zone of ductile flow in the middle- and lower-‘crust’. Experiments with a thinner ductile ‘crust’ show a more symmetrical pattern of shear zones in the middle and upper ductile ‘crust’ and brittle upper ‘crust’ than models with an initially thicker ductile ‘crustal’ sequence. A thin ductile crust therefore couples deformation between the mantle lithosphere and upper brittle crust whereas a thicker ductile crust decouples the two units. Displacement may even be greater on basin-bounding faults that are antithetic to a deeper ‘crustal’ shear zone for part of the basin formation. Basins may show a flip in polarity, with later stages being controlled by a synthetic fault.

Distinct structural features are developed at different levels in the crust due to differing rheology and proximity to other deforming layers. If a shear zone develops early in the ductile ‘crustal’ layers, then deformation will remain concentrated within it. Minor conjugate normal shear zones are produced in the ductile ‘crust’, on the boundary of the uplifted ‘mantle lithosphere’ footwall, and on the flank of the ‘mantle asthenosphere’ ridge. Uplift of ‘mantle lithosphere’ results in a flattening of the dip of early-formed ductile shear zones. Such shear zones may change in profile

from concave upward in the ductile ‘crust’ to convex upward at deeper levels.

Several folding mechanisms coexist. Upright antiforms (e.g. layer 7 in Fig. 6b and d) and synforms (e.g. layers 1 and 2, centre of Fig. 5c) develop due to flow of ductile layers into boudin necks. Some folds initiate as upright to inclined structures above the crest of the uplifted ‘mantle lithosphere’ footwall (e.g. layer 1, Fig. 4b). This has occurred irrespective of the initial inclination of the prescribed cut through the ‘mantle lithosphere’ layer. Upright folds are progressively rotated to inclined or recumbent attitudes with progressive deformation by displacement on normal shear zones (e.g. Fig. 4d and f). Their lower limbs are highly attenuated and may sole out onto sub-horizontal shear zones. High shear strains occur in normal shear zone above the shallowly dipping rotated footwall to the pre-existing fault in the ‘mantle lithosphere’. Some folds within these ductile shear zones may form in an original, shallow orientation (e.g. folds in layer 1 in left side of Fig. 6a). Folds also nucleate due to irregularities in the footwall surface of the ‘mantle lithosphere’ (Fig. 7a–c, e and f). Stratigraphic repetition and complex fold-nappe style geometries may be produced (e.g. Figs. 4f and h and 5j). Folds are developed through a greater section of the crust in the case of a thinner ductile crust and shallower dip of the prescribed cut (Model 2). Open folds of competent layers in the ductile ‘crust’ of our models have also formed due to drag into normal shear zones (e.g. layer 3 in Figs. 5g and 7e and f and layer 6 in Fig. 7a). Early-formed recumbent folds may be refolded due to either uplift of the ‘asthenosphere’ (e.g. Figs. 4h and 7b), or due to interference by later upright folds formed at a higher level in the crust between boudinaged competent layers (e.g. Fig. 5j).

The lateral extent of folds varies depending on the dip of the ‘mantle shear zone’. When the shear angle is high, the two competent units, upper crust and lithosphere, are coupled, which means that deformation within the ductile unit between them is concentrated to a narrow area. When the shear zone dips gently, and rotates to even gentler dip during extension, the two units are decoupled by the ductile lower crust. In this case, movement along the lithosphere shear zone is accommodated by ductile flow within a wider zone. As extension continues, the shear zone rotates and shifts position. As the shear zone shallows in dip, movement along it becomes sub-parallel to the layering in the ‘lower crust’, resulting in both a wider deformation area and folds with large lateral extent. Both processes lead to involvement of a wider zone of the lower crust in the deformation.

Similar structures to those developed in our models also form in layered gneiss at the outcrop scale, such as folds from the Norwegian Caledonides illustrated by Fossen and Rykkelid (1992) and Harris et al. (2002). Structures in models likewise resemble those produced in a thrust/convergent margin tectonic setting, or due to gravitational spreading at an upper structural level (Brun and Merle, 1988). A major difference between our models and

‘alpine-style’ nappe structures is the lack of deformation in the overlying crustal layers in our models.

## 5.2. Differences and similarities between analogue models and nature

Some limitations are inherent in our models. All models in this experimental program have comprised relatively thick competent layers within the ductile ‘crust’. In nature, the structures developed may be of proportionally smaller size as competent horizons are thinner. Changes in the position of competent layers, their thickness or their complete removal would be likely to produce different fold geometries. Further experiments with different strength profiles, and without the pre-existing cut in the mantle lithosphere are planned to fully develop the potential of this method. The materials used do not allow the formation of a new foliation during deformation, as may be expected in nature. The flattening and elongation of bubbles trapped during layer construction (as seen in Figs. 5 and 6), however, gives an indication that a flattening foliation may be expected to develop and be subsequently deformed.

In nature, an anastomosing network of shear zones in the upper mantle may form during initial stretching prior to development of a shear zone that cuts the mantle lithosphere (Froitzheim and Manatschal, 1996). The presence of a pre-existing cut through the mantle lithosphere layer inhibits such early pure shear deformation in the models presented in this paper. Despite strain localization due to the presence of an initial cut, considerable necking of the mantle lithosphere layer has, however, taken place in some experiments (e.g. right hand side of Fig. 4a and g). Boudinage of the mantle lithosphere layer has occurred in Model 2 (Fig. 5c).

It has not been possible to include the effects of increased heat-flow in a rift zone in our models. In nature, a new lithospheric mantle would be established in the region of asthenospheric uplift (as portrayed by Froitzheim and Manatschal, 1996). Where mantle asthenosphere is bowed upward during asymmetric extension, partial melting of the mantle and lower crust may occur, along with mafic underplating at the base of the thinned crust. An example of this process comes from the central Fennoscandian Shield where a three-dimensional crustal geometry has been obtained from reflection seismic profiles (Korja and Heikkinen, 1995). Mantle-derived igneous intrusions may be localised in the thinned lower crust above boudin necks in the mantle lithosphere (such as in Fig. 5c). At higher strain where the mantle lithosphere has separated, more voluminous AMCG-suite rocks (anorthosites, mangerites, charnockites and granitoids, including rapakivi granites) may intrude the lower crust above asthenospheric domes (as portrayed by Kazansky, 1995, fig. 117). Intrusion of these bodies may further deform earlier structures.

In spite of these differences, comparisons with deep seismic profiles and field examples of structures in extensional amphibolite and granulite facies terrains suggest that

structures akin to those seen in our models exist in nature (see review by Harris et al., 2002). For example, the deep crustal structure of the Rhine Graben interpreted by Brun et al. (1992) from DEKORP-ECORS seismic reflection data is identical to early stages of our models. Kilometre-scale recumbent folds and boudins in the Ruby Mountains have been attributed to mid-crustal flow during Tertiary extension by MacCready et al. (1997). Recumbent fold nappes that have undergone subsequent doming in West Greenland portrayed by Escher and Pulvertaft (1976) may also be the product of ductile flow during crustal extension. A major advantage of our models is that they show the initiation, progressive evolution and mutual interference of structures.

The results of this study are applicable to regions that have developed through a prior stage of continental collision where a discontinuity (e.g. a former subduction zone) is likely to be present in the mantle lithosphere prior to the onset of rifting. This would equate to the initial cut made through the mantle lithosphere layer in the centrifuge models. It is common for rifts to develop along older orogenic belts, such as the Permo–Triassic ‘Gondwanan’ rift basins that reactivate Proterozoic orogenic belts across Gondwanaland (Daly et al., 1989; Harris, 1994). Extensional reactivation of deep-seated weaknesses may be due to: (i) far-field stresses of a convergent orogen (Daly et al., 1989; Harris, 1994), (ii) tensile in-plate stresses due to slab pull at distant subduction zones (Zoback et al., 1989), or (iii) mantle plumes (Harris, 1996). The latter mechanism is not appropriate to these experiments, as no such plume perturbation was included in model construction.

### 5.3. Comparison with other conceptual models of lower crustal flow

Our centrifuge models show initial displacement along a shear zone displacing the ‘lithospheric mantle’ layer. Greater extension results in separation of the ‘mantle lithosphere’ layer and doming of the ‘asthenosphere’, thereby juxtaposing ‘asthenosphere’ and lower ‘crust’. Wernicke’s (1990) model for extensional tectonism of a lithosphere containing a flowing, ductile crustal layer also suggests that the mantle lithosphere may be separated along a mantle shear zone at high strain. In his model, the top of the mantle lithosphere hanging wall appears to be at only a slightly greater depth than the footwall, and the Moho is generally flat. In our experiments, however, a greater amount of normal displacement has taken place prior to separation and asthenospheric upwelling. Our centrifuge experiments substantiate Wernicke’s (1990) conceptual model that shows that the ‘mantle lithosphere’ footwall has been rotated to a sub-horizontal attitude. Both show a zone of ductile shearing above the rotated footwall mantle discontinuity. Although the geometry of the lowermost ‘crust’, ‘mantle lithosphere’ and ‘asthenosphere’ in our models is similar to that of the conceptual model of Wernicke (1990), our experiments show a thickened ‘syn-rift’ section above

the rift axis. Wernicke’s (1990) model has a thinning of the brittle crust and no syn-rift sediments above the elevated asthenosphere. This could be due to thermal buoyancy, which is lacking in our models described here. However, in nature, a thermal uplift is followed by a thermal subsidence when asthenosphere cools.

In deep seismic interpretations for the North Sea, the extensional shear zones cutting the upper mantle do not directly link with faults in the upper crust. Kuszniir and Matthews (1988), Wernicke (1990), Reston (1990), Blundell (1990) and Brun and Tron (1993) all conclude that there has been decoupling between upper crust and mantle. This agrees with Kuszniir and Matthews’ (1988) view that there are no clearly documented cases where a low angle fault passes continuously from the surface through the entire crust and into the mantle (as in the simple shear model of Wernicke, 1985). The lower crust has acted as a divide between localised deformation in the upper crust and in the lithospheric mantle, implying lower crustal ductile flow during rifting, as produced in the centrifuge models described above.

## 6. Conclusions

The results of centrifuge modelling have provided new insights into the progressive development of structures likely to occur in high-grade rocks due to ductile flow during extension of continental lithosphere. Models suggest that during rifting, the upper brittle crust may deform in an extremely simple manner whilst the middle and lower ductile crust may undergo complex deformation, including the formation of refolded recumbent folds. Although not modelled in the present study, similar structures in the lower ductile crust may also be expected to develop during collapse of a thrust-thickened collisional orogen. This study highlights the need for extreme care to be taken in basing interpretations of tectonic setting and relative timing of deformation in high-grade gneiss terrains on fold style and geometry. It suggests that one may need to re-examine previous contractional, convergent-margin tectonic interpretations for some high-grade metamorphic terrains.

## Acknowledgements

Research was funded by the Swedish Institute (to Koyi and Harris) and an Australian Research Council Small Grant (to Harris). C. Talbot is thanked for his advice and general discussions. L. Kriegsman and C. Wilson are thanked for their detailed reviews and helpful suggestions, and A. Gartrell for comments on an earlier draft. G. Mulugeta provided some of the materials used for modelling the brittle crust and assistance in viscosity measurements. HAK is funded by the Swedish Research Council (VR). This is Tectonics Special Research Centre publication number 174.

## References

- Artemieva, I.M., Mooney, W.D., 2001. Thermal thickness and evolution of Precambrian lithosphere: a global study. *Journal of Geophysical Research* B8, 16387–16414.
- Benes, V., Davy, P., 1996. Modes of continental lithospheric extension: experimental verification of strain localization processes. *Tectonophysics* 254, 69–87.
- Blundell, D.J., 1990. Relationships between deep crustal structure and sedimentary basins around Britain. In: Pinet, B., Bois, C. (Eds.). *The Potential of Deep Seismic Profiling for Hydrocarbon Exploration*. Editions Technip, Paris, pp. 317–333.
- Boger, S.D., Carson, C.J., Wilson, C.J.L., Fanning, C.M., 2000. Neoproterozoic deformation in the Radok Lake region of the northern Prince Charles Mountains, East Antarctica; evidence for a single protracted orogenic event. *Precambrian Research* 104, 1–24.
- Boutillier, R.R., Keen, C.E., 1994. Geodynamic models of fault-controlled extension. *Tectonics* 13, 439–454.
- Brun, J.-P., Merle, O., 1988. Experiments on folding in spreading–gliding nappes. *Tectonophysics* 145, 129–139.
- Brun, J.-P., Tron, V., 1993. Development of the North Viking Graben: inferences from laboratory modelling. *Sedimentary Geology* 86, 31–51.
- Brun, J.-P., Beslier, M.O., 1996. Mantle exhumation at passive margins. *Earth and Planetary Science Letters* 142, 161–173.
- Brun, J.-P., Gutscher, M.A., DEKORP-ECORS teams, 1992. Deep crustal structure of the Rhine Graben from DEKORP-ECORS seismic reflection data: a summary. *Tectonophysics* 208, 139–147.
- Buck, W.R., 1988. Flexural rotation of normal faults. *Tectonics* 7, 959–973.
- Buck, W.R., 1991. Modes of continental lithospheric extension. *Journal of Geophysical Research* 96, 20161–20178.
- Buck, W.R., Martinez, F., Steckler, M.S., Cochran, J.R., 1988. Thermal consequences of lithospheric extension: pure and simple. *Tectonics* 7, 213–234.
- Daly, M.C., Chorowicz, J., Fairhead, J.D., 1989. Rift basin evolution in Africa: the influence of reactivated steep basement shear zones. In: Cooper, M.A., Williams, G.D. (Eds.), *Inversion Tectonics*. Geological Society of London Special Publication 44, pp. 309–334.
- Dixon, J.M., Summers, J.M., 1985. Recent developments in centrifuge modelling of tectonic processes: equipment, model construction techniques and rheology of model materials. *Journal of Structural Geology* 7, 83–102.
- Escher, A., Pulvertaft, T.C.R., 1976. Rinkian mobile belt of West Greenland. In: Escher, A., Stuart Watt, W. (Eds.). *Geology of Greenland*. Geological Survey of Greenland, pp. 105–119.
- Fernández, M., Ranalli, G., 1997. The role of rheology in extensional basin formation modelling. *Tectonophysics* 282, 129–145.
- Fossen, H., Rykkelid, E., 1992. The interaction between oblique and layer-parallel shear in high-strain zones: observations and experiments. *Tectonophysics* 207, 331–343.
- Froitzheim, N., Manatschal, G., 1996. Kinematics of Jurassic rifting, mantle exhumation, and passive-margin formation in the Austroalpine and Penninic nappes (eastern Switzerland). *Geological Society of America Bulletin* 108, 1120–1133.
- Gartrell, A.P., 2000. Modes of extension, mobility of the lower crust and the structural evolution of the North West Shelf. *Australian Journal of Earth Sciences* 47, 231–244.
- Govers, R., Wortel, M.J.R., 1993. Initiation of asymmetric extension in continental lithosphere. *Tectonophysics* 223, 75–96.
- Govers, R., Wortel, M.J.R., 1995. Extension of stable continental lithosphere and the initiation of lithosphere scale faults. *Tectonics* 14, 1041–1055.
- Harris, L.B., 1994. Structural and tectonic synthesis for the Perth Basin. *Western Australia. Journal of Petroleum Geology* 17, 129–156.
- Harris, L.B., 1996. Polyphase faulting in the Perth Basin and Yilgarn Craton, Western Australia: relationship to Upper Paleozoic–Mesozoic tectonics of Gondwanaland. In: Guha, P.K.S., Ayyasami, K., Sengupta, S., Ghosh, R.N. (Eds.), *Gondwana 9*. Oxford and IBH Publishing 2, pp. 1051–1060.
- Harris, L.B., Koyi, H.A., Fossen, H., 2002. Mechanisms for folding of high-grade rocks in extensional tectonic settings. *Earth Science Reviews* in press.
- Hopper, J.R., Buck, W.R., 1996. The effect of lower crustal flow on continental extension and passive margin formation. *Journal of Geophysical Research* B 101, 20175–20194.
- Kazansky, V.I., 1995. Evolution of Ore-bearing Precambrian Structures. IUGS-UNESCO IGCP Project 247. Russian Translation Series 110. Balkema, Rotterdam.
- Keen, C.E., Boutillier, R.R., 1990. Geodynamic modelling of rift basins: the syn-rift evolution of a simple half-graben. In: Pinet, B., Bois, C. (Eds.). *The Potential of Deep Seismic Profiling for Hydrocarbon Exploration*. Editions Technip, Paris, pp. 23–33.
- Klemperer, S., 1988. Crustal thinning and the nature of extension in the North Sea from deep seismic reflection profiling. *Tectonics* 7, 803–821.
- Korja, A., Heikkinen, P.J., 1995. Proterozoic extensional tectonics of the Fennoscandian Shield: results from the Baltic and Bothnian Echoes from the Lithosphere experiment. *Tectonics* 14, 504–517.
- Koyi, H.A., Skelton, A., 2001. Centrifuge modelling of the evolution of low-angle detachment faults from high-angle normal faults. *Journal of Structural Geology* 23, 1179–1185.
- Koyi, H.A., Harris, L.B., 2001. Spatial and temporal migration of basin depocenters above low-angle detachments; a centrifuge-model approach. *Energy Exploration and Exploitation*, 19, 365–374.
- Kruse, S., McNutt, M., Phipps-Morgan, J., Royden, L., Wernicke, B., 1991. Lithospheric extension near Lake Mead, Nevada: a model for ductile flow in the lower crust. *Journal of Geophysical Research* B96, 4435–4456.
- Kusznir, N.J., Park, R.G., 1984. Intraplate lithospheric deformation and the strength of the lithosphere. *Geophysical Journal of the Royal Astronomical Society* 79, 513–538.
- Kusznir, N.J., Matthews, D.H., 1988. Deep seismic reflections and deformational mechanics of the continental lithosphere. *Journal of Petrology, Special Lithosphere Issue*, 63–87.
- Lister, G.S., Etheridge, M.A., Symonds, P.A., 1986. Detachment faulting and the evolution of passive continental margins. *Geology* 14, 246–250.
- Lister, G.S., Etheridge, M.A., Symonds, P.A., 1991. Detachment model for the formation of passive continental margins. *Tectonics* 10, 1038–1064.
- McClay, K.R., 1976. The rheology of plasticine. *Tectonophysics* 33, T7–T15.
- MacCready, T., Snoko, A.W., Wright, J.E., Howard, K.A., 1997. Mid-crustal flow during Tertiary extension in the Ruby Mountains core complex, Nevada. *Geological Society of America Bulletin* 109, 1576–1594.
- Meissner, R., Wever, T., 1988. Lithospheric rheology: continental versus oceanic unit. *Journal of Petrology, Special Lithosphere Issue*, 53–61.
- Melosh, H.J., 1990. Mechanical basis for low-angle normal faulting in the Basin and Range Province. *Nature* 343, 331–335.
- Mooney, W.D., Meissner, R., 1992. Multi-genetic origin of crustal reflectivity: a review of seismic profiling of the continental lower crust and Moho. In: Fountain, D.M., Arculus, R., Kay, R.W. (Eds.), *Continental Lower Crust*. Development in Geotectonics 23, pp. 45–79.
- Passchier, C.W., Myers, J.S., Kroner, A., 1990. *Field Geology of High-grade Gneiss Terrains*. Springer-Verlag, Berlin, New York.
- Phinney, R.A., 1986. A seismic section of the New England Appalachians: the orogen exposed. In: Barazangi, M., Brown, L.D. (Eds.), *Reflection Seismology: The Continental Crust*. American Geophysical Union Geodynamic Series 14, pp. 157–172.
- Poudjom Djomani, Y.H., O'Reilly, S.Y., Griffin, W.L., Morgan, P., 2001. The density structure of subcontinental lithosphere through time. *Earth and Planetary Science Letters* 184, 605–621.
- Ramberg, H., 1967. Gravity, Deformation, and the Earth's Crust as Studied by Centrifuged Models. 1st ed. Academic Press, London, New York.
- Ramberg, H., 1973. Model studies of gravity-controlled tectonics by the

- centrifuge technique. In: de Jong, K.A., Scholten, R. (Eds.). *Gravity and Tectonics*. Wiley-Interscience, pp. 49–66.
- Ramberg, H., 1981. *Gravity, Deformation, and the Earth's Crust in Theory, Experiments, and Geological Application*. 2nd ed. Academic Press, London, New York.
- Ranalli, G., 1997. Rheology of the lithosphere in space and time. In: Burg, J.P., Ford, M. (Eds.), *Orogeny Through Time*. Geological Society of London Special Publication 121, pp. 19–37.
- Reston, T.J., 1990. The structure of the crust and uppermost mantle offshore Britain: deep seismic reflection profiling and crustal cross-sections. In: Salisbury, M.H., Fountain, D.M. (Eds.), *Exposed Cross-sections of the Continental Crust*. Kluwer Academic, pp. 603–621.
- Reston, T.J., 1993. Evidence for extensional shear zones in the mantle, offshore Britain, and their implications for the extension of the continental lithosphere. *Tectonics* 12, 492–506.
- Sandiford, M., Wilson, C.J.L., 1984. The evolution of the Fyfe Hills–Khmara Bay region, Enderby Land, East Antarctica. *Australian Journal of Earth Sciences* 31, 403–426.
- Schellart, W.P., 2000. Shear test results for cohesion and friction coefficients for different granular materials: scaling implications for their usage in analogue modelling. *Tectonophysics* 324, 1–16.
- Vissers, R.L.M., Drury, M.R., Hoogerduijn-Strating, E.H., Spiers, C.J., van der Wal, D., 1995. Mantle shear zones and their effect on lithosphere strength during continental breakup. *Tectonophysics* 249, 155–171.
- Vissers, R.L.M., Drury, M.R., Newman, J., Fliervoet, T.F., 1997. Mylonitic deformation in upper mantle peridotites of the North Pyrenean Zone (France); implications for strength and strain localization in the lithosphere. *Tectonophysics* 279, 303–325.
- Warner, M., McGeary, S., 1987. Seismic reflection coefficients from mantle fault zones. *Geophysical Journal of the Royal Astronomical Society* 89, 223–230.
- Weijermars, R., 1986. Flow behaviour and physical chemistry of bouncing putties and related polymers in view of tectonic laboratory applications. *Tectonophysics* 124, 325–358.
- Weijermars, R., 1997. *Principles of Rock Mechanics*. Alboran Science Publishing, Amsterdam.
- Weijermars, R., Schmeling, H., 1986. Scaling of Newtonian and non-Newtonian fluid dynamics without inertia for quantitative modelling of rock flow due to gravity (including the concept of rheological similarity). *Physics of the Earth and Planetary Interiors* 43, 316–330.
- Wernicke, B., 1985. Uniform-sense normal simple shear of the continental lithosphere. *Canadian Journal of Earth Sciences* 22, 108–125.
- Wernicke, B., 1990. The fluid crustal layer and its implications for continental dynamics. In: Salisbury, M.H., Fountain, D.M. (Eds.), *Exposed Cross-sections of the Continental Crust*. Kluwer Academic, pp. 509–544.
- Westaway, R., 1998. Dependence of active normal fault dips on lower-crustal flow regimes. *Journal of the Geological Society of London* 155, 233–253.
- Zoback, M.L., Zoback, M.D., Adams, J., Assumpção, M., Bell, S., Bergman, E.A., Blümling, P., Breerton, N.R., Denham, D., Ding, J., Fuchs, K., Gay, N., Gregersen, S., Gupta, H.K., Gvishiani, A., Jacob, K., Knoll, P., Magee, M., Mercier, J.L., Müller, B.C., Paquin, C., Rajendran, K., Stephansson, O., Suarez, G., Suter, M., Udias, A., Xu, Z.H., Zhizhin, M., 1989. Global patterns of tectonic stress. *Nature* 341, 291–298.
- Zuber, M.T., Parmentier, E.M., Fletcher, R.C., 1986. Extension of the continental lithosphere: a model for two scales of Basin and Range deformation. *Journal of Geophysical Research* B 91, 4826–4838.